Direct Registration of White Matter Tractographies with Application to Atlas Construction

Arnaldo Mayer, Hayit Greenspan

Medical image processing lab, Tel-Aviv University, Ramat-Aviv, Israel
arnakdom@post.tau.ac.il, hayit@eng.tau.ac.il

Abstract. We present a new method for direct inter and intra-subject registration of White Matter (WM) tractographies. The method does not require any previous registration between the brains, such as DTI registration. The algorithm is inspired by the well known iterative closest point method. Here, 3D points are replaced by feature vectors representing WM fibers, and the neighborhood is determined by the efficient approximation framework of the locality sensitive hashing. Initial results demonstrate the successful application of the proposed method to the automatic extraction and registration of the Corticospinal tract (CST) from un-segmented tractographies for the construction of a probabilistic atlas.

Keywords. MRI, Brain, Tractography, Registration, Atlas.

1 Introduction

In the last ten years, Diffusion Tensor Imaging (DTI) is changing the way we perceive White Matter (WM) in MRI brain [1]. From a set of Diffusion Weighted Images (DWI), a distinct diffusion tensor is computed and assigned to each voxel. The principal directions of the tensor were shown to generally coincide with the local orientation of sub-voxels WM axons bundles [2]. Many algorithms, deterministic and stochastic, were devised to propagate the principal direction of diffusion from seed voxels to the whole brain WM [2]. This enabled impressive in-vivo reconstructions of major WM tracts [3]. Sophisticated freeware packages have become available on the web, for tensor computation and tractographic reconstruction on DWI data [4,5]. Recently, a set of probabilistic atlases that average main tracts itineraries over many co-registered tractographies were published on the website of Johns Hopkins Medical MRI Laboratory [6]. Clustering based methods were also proposed for the modeling of fiber tracts by a Gaussian mixture ([7]) or through normalized cuts ([8]). In all these prior works, pre-registration between the brains was a necessary condition for the atlas construction. The main contribution of the current paper is to propose and demonstrate a robust and efficient method for direct registration and matching between tractographic fiber sets without requiring prior registration of the original

MRI or DTI scans. The proposed method is applied to the construction of a probabilistic atlas for the CST. The rest of this paper is organized as follows: In section 2 we describe the proposed algorithm. The application to the construction of an atlas is presented in section 3. Conclusions follow in section 4.

2 Algorithm Description

Denote by M_i,$i=1..n$ and T_j, $j=1..m$ a model and target set of fibers, respectively. Each fiber is described by a sequence of 3D coordinates describing its trajectory between the extremities it connects. In this work, the sets M and T are obtained by tractographic reconstruction of the DTI data using DtiStudio. The model and target sets may originate from the same brain, as in the case of intra-subject registration for longitudinal studies. Alternatively, the sets may belong to distinct brains for inter-subject registration. For the target set, we will consider all the WM fibers reconstructed by tractography. For the model set we can consider any anatomical tract of interest, in example the CST. Our goal is to match between model and target fibers by finding for each model fiber M_i, the target fiber T_j that best corresponds. At the same time, we want to perform spatial registration between the corresponding fiber sets. If we think of a fiber as a point in some feature space, the matching-registration problem can be viewed as a (feature) point sets matching-registration. We adopt this approach by extending the well known iterative closest point (ICP) algorithm for 3D point sets [9] to an iterative closest fiber (ICF) algorithm for tractographic fiber sets. The main ICF steps are: 1) Represent each model and target fiber by a distinct feature vector. 2) For each model fiber M_i find the "closest", that is most similar, target fiber T_j. 3) Given the set of fiber correspondences found in 2), fit a linear geometric transformation between model and target fibers. 4) Warp the model fiber set using the transformation computed in 3). 5) Repeat from point 2) until convergence or a maximum number of iterations is reached. 6) Return the final correspondence set between model and target fibers together with the combined geometric transform between original (non-warped) model and target sets.

2.1 Fiber representations

We now define two feature space representations of the fibers that will be motivated and used in the following steps of the algorithm:

I) Spatial Coordinates Sequence
The fibers generated by DtiStudio are represented by a variable number of points. Therefore, we re-sample each fiber f along its trajectory at a fixed number n of uniformly distributed points. Each fiber is now represented by the same number of points n. By linearly appending the re-sampled coordinate sequence, (x_{Sj},y_{Sj},z_{Sj}), we obtain the *1x3n* feature vector :

$$f_{CS} = [x_{s_1}, y_{s_1}, z_{s_1}, \ldots, x_{s_n}, y_{s_n}, z_{s_n}] \ . \quad (1)$$

II) Direction vectors sequence

An alternative representation is derived from the preceding one, by replacing every two successive points in the feature vector with the unit direction vector (u_{Sj}, v_{Sj}, w_{Sj}) they define. Note that *n* sample points defining a fiber in the previous representation will result in *n-1* unit direction vectors. The corresponding *1x(3n-1)* feature vector is obtained, as before, by linearly appending the direction vectors sequence:

$$f_{ds} = [u_{s_1}, v_{s_1}, w_{s_1}, \ldots, u_{s_{n-1}}, v_{s_{n-1}}, w_{s_{n-1}}] \ . \tag{2}$$

Note that (2) is inherently a shift and scale invariant representation of a fiber.

2.2 Fiber Similarity

The definition of fiber similarity is a critical issue for the success of the ICF algorithm. Consider a given pair M_i, T_j of corresponding model-target fibers before the first iteration. For the sake of simplicity we will consider that both model and target sets are extracted from the same brain. Since M_i and T_j are corresponding fibers, we must have:

$$\arg\max_n \left(S(M_i, T_n)\right) = j \ . \tag{3}$$

where S is an appropriate fiber similarity function. At this stage, however, the relative orientation, position and scale differences between model and target sets are still arbitrary. Therefore, S should mainly rely on shape to provide a meaningful similarity score. We define *R(U,V)*, the vector correlation coefficient (VCC) between two 3-dimensional random vectors $U=(u_x, u_y, u_z)$ and $V=(v_x, v_y, v_z)$ on a unit sphere, as [10]:

$$R(U,V) = \frac{\det(n^{-1}\sum_{i=1}^{n} U_i V_i^{\,t})}{\{\det(n^{-1}\sum_{i=1}^{n} U_i U_i^{\,t})\det(n^{-1}\sum_{i=1}^{n} V_i V_i^{\,t})\}^{1/2}}, \qquad -1 \le R \le 1 \ . \tag{4}$$

where U_i, and V_i are the sequences of n realizations of random vectors *U* and *V*, respectively. For strong correlation, *R* approaches +1 if the sequences are in the same order and R approaches -1 if the sequences are in reversed order (reflection). As correlation decreases, *abs(R)* moves towards 0. The feature vector of (2) is actually a sequence of unit direction vectors, therefore it can be viewed as a sequence of random vectors on a unit sphere and we can compute the VCC between any pair of model and target fibers represented by (2). The VCC is shown to be rotation invariant [10]. The shift and scale invariance of (2) combined with rotation invariance of the VCC are particularly useful for the first iteration of the ICF algorithm, when the fiber sets are still arbitrarily misaligned. On the other hand, when iterations proceed and misalignment progressively decreases, position orientation and scale information may be important in order to increase the specificity of the similarity function. For example, let's suppose that a given fiber shape appears in several identical instances in the target brain but at slightly different positions or orientations. A fiber similarity

measurement exclusively based on the VCC would be indifferent to these position\orientation shifts, making the preferred match ambiguous and limiting the matching accuracy. At the first iteration, VCC robustness to large misalignment prevails over its limitations. As misalignment decreases, however, trading up VCC invariance for more specific L_2 distance leads to higher matching accuracy. This suggests a two-fold strategy for fiber similarity measurement. For the first iteration we take as similarity function, S, the VCC between model and target fibers in the feature vector representation of (2). We delimit the range of tolerated position, orientation and scaling misalignment, *(DP,DR,DS)* by multiplying VCC with a threshold function, *TF(DP,DR,DS)*, that forces S to zero for extreme misalignments:

$$S^{it=1}(M_i,T_j) = abs(\rho(f_{ds}(M_i), f_{ds}(T_j))) * \mathrm{TF}(DP,DR,DS), \qquad 0 \le S^{it=1} \le 1 \ . \qquad (5)$$

For the following iterations, we define S as a decreasing function of the normalized L_2 distance between model and target fibers in the feature vector representation of (1):

$$S^{it>1}(M_i,T_j) = 1 - \frac{\left\| f_{cs}(M_i) - f_{cs}(T_j) \right\|_2}{C}, \qquad 0 \le S^{it>1} \le 1 \ . \qquad (6)$$

Where C is a normalizing constant. In practice, as we look for the nearest target fiber for every model fiber, we replace the naïve computation of L_2 distances with a fast approximate nearest-neighbor (NN) computation provided by the locality sensitive hashing framework (LSH) [11]. With LSH, the target data is embedded in the bins of several hash tables in a pre-processing step. The hash functions have the property of assigning neighboring feature points to the same bins with an elevated probability [11]. The resulting speed-up with regard to naïve NN computation is of at least two orders of magnitude in our application for fibers typically represented by 60-dimensional feature vectors.

2.3 Geometric Transformation Fitting

At each ICF iteration we estimate a 12 parameters 3D affine transformation that best warps, in the least squares sense, the model fibers set into the corresponding target fibers found in the previous step. The choice of the affine transform is motivated by our goal of matching corresponding fibers from the model and target sets. For this purpose we need enough flexibility to compensate for global orientation, position and (per-axis) scale differences between the sets. The affine model offers this flexibility while remaining very easy to fit. Higher order transforms can be considered to allow for local deformations. For fiber matching however, perfect warping between model and target fiber is not required. Similarly, when building a statistical WM atlas from a number of aligned tracts, local deformations would discard precious inter-subject variability information. We implement the affine transform fitting using the RANSAC [12] method to ensure robustness against outliers. The Flow diagram in figure 1, summarizes the ICF algorithm described above.

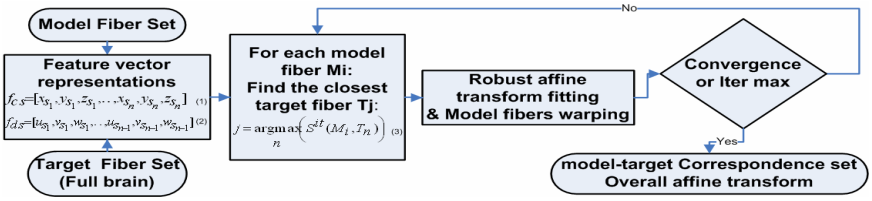

Fig. 1 ICF algorithm.

3 Experiments

In this section we describe the application of the presented method to the construction of a probabilistic atlas for the CST. The atlas construction is an inter-subject registration scenario as it requires many pair-wise registrations between different brain's CST and a reference model.

3.1 The data

The data set consists of 15 normal brains downloaded from Johns Hopkins Medical MRI Laboratory website [6]. Each brain is represented by 50-55 axial slices with a voxel size of 1x1x2.6 mm in the x,y,z directions respectively. Figure 2 shows the fractional anisotropy for the mid-scan slices extracted from brains number 1(left), 5(middle), and 11(right) of the dataset. The initial misalignment between the brains is clearly observable. The full brain white matter tractography is generated for each one of the 15 brains using DtiStudio. In this experiment we take as reference model the CST of brain number 1. In order to build the probabilistic atlas, we need to align the CST of the remaining 14 brains with the model. The model CST is extracted manually from the tractography of the first brain using the interactive region of interest tools provided by DtiStudio. Figure 3 shows the fibers of the CST model in overlap with brain number 1 in sagittal (left) and coronal (right) views. Actually the anatomical accuracy of the selected model relies on the neuro-anatomist skills in extracting the relevant fibers and it is not an objective of this experiment. The obtained reference CST has 1055 fibers while the other 14 brains have 200-250 K fibers each. All the fibers are re-sampled to have n=20 representative points, leading to a 57-dimensional f_{ds} and a 60-dimensional f_{cs} feature vectors per fiber. The spatial coordinates in f_{cs} feature vectors were converted to mm and then normalized to a unit less [0,1] range for the three axes.

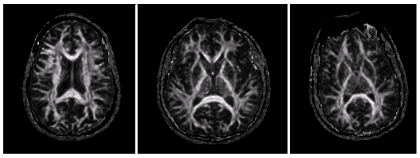

Fig. 2 Fractional anisotropy for the mid-scan slice for brain number 1(left); 5(middle); 11(right).

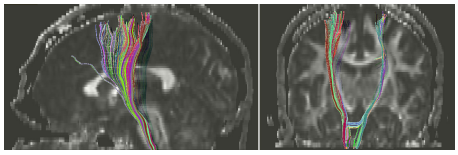

Fig. 3 Fibers of the CST model in overlap with brain number 1 in sagittal (left) and coronal (right) views.

3.2 Atlas Generation

The ICF algorithm is applied between the model CST (of the first brain) and the full tractography of each of the remaining 14 brains, hereafter termed target fibers. We choose an affine warping between fibers in order to keep and integrate inter-subjects anatomical variability into the atlas. The maximal number of iterations is set to 15. Iterations are stopped anyway if no fiber re-assignment occurs during any iteration. In the ICF iteration, it may happen that two or more model fibers should be associated to the same target fiber, relying on the minimum distance criterion. For the atlas construction, however, we are interested in finding as many as possible corresponding target fibers. Therefore instead of assigning many model fibers to the same target fiber, we assign each model fiber to the closest target fiber that has no better matching options. This can result in matching between the first, second, or even k-nearest neighbors. To avoid meaningless matching between fairly different fibers the maximal distance for matching is limited empirically to 20% of the normalized feature vector f_{CS} dimensionality (which is 60 in our case). The maximal number of considered nearest neighbors, k, is limited to 60 for computation time considerations.
In figure 4, we show the results of the ICF registration for brain number 5 (top row) and number 11 (bottom row). Figures 4(a,b) show the matched target fibers before the registration warping (red) together with the corresponding model fiber (green) in frontal (a) and top (b) views. Figures 4(c,d) show the same target fibers (red) warped by the ICF affine transforms to match their corresponding model (green) fibers in frontal (c) and top (d) views. Note that although the affine warping has compensated for the global misalignment, the anatomical specificities of the model-target tracts are still apparent. In figure 5(a), we compare the mean squared error between model and target fibers before (red curve) and after (green curve) registration with the ICF for each brain in the dataset. The ICF has reduced the remaining MSE in the range of 1/5 to 2/5 of its initial value. Moreover, the ICF was able, for every considered brain, to extract automatically the CST out of the whole WM tractography although the CST represented only about 0.5% of the total number of fibers. Figure 5(b) shows the 14 target CSTs after their alignment with the model, each color representing another brain from the dataset. Finally, a probabilistic map or atlas for the CST is generated by writing in each voxel of brain number 1 axes the number of aligned CST fibers that passes through that voxel. The voxels are then normalized to sum up to one. Figure 6 shows the coronal slices number 113 (top left) to 133 (bottom right) of the CST atlas. The Probability of a voxel to belong to the CST is represented by its red color intensity.

4 Conclusions

We have presented a new robust and efficient method for direct registration and matching of tractographic fiber sets without requiring any previous registration step of the original MRI scans. Initial results were presented for the automatic extraction and registration of the CST in un-segmented tractographies. The registered tracts were combined into a probabilistic atlas for the CST. The method showed promising results. In its current Matlab implementation, the running time for each model-target registration is in the 30-45 minutes range. The ICF running time would certainly improve in a C/C++ implementation. In the continuation of this work we will investigate the optimal fiber representation length for the ICF algorithm. Intuitively, representation length should increase with the order of the geometric transformation. Since ICF computation time also increases with representation length, the optimal length should reflect a trade-off between desired registration accuracy and computation time. We also intend to apply the method to other WM tracts, generate atlases in standard spaces such as MNI and extend them to larger datasets.

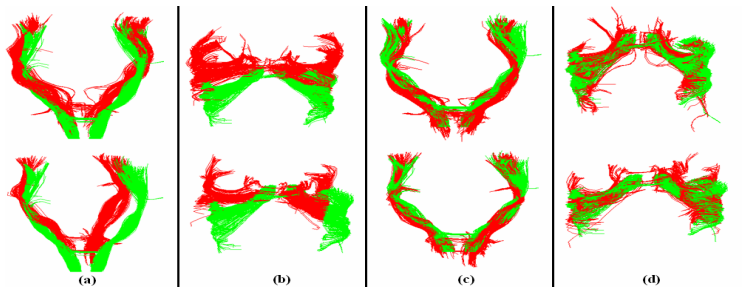

Fig. 4 (a) matched target fibers before the registration warping (red) together with corresponding model fibers (green) in frontal view; (b) in top view; (c) same target fibers (red) warped by the ICF affine transforms to match their corresponding model (green) fibers in frontal view; (d) in top view. Top and bottom rows show target brains number 5 and 11, respectively.

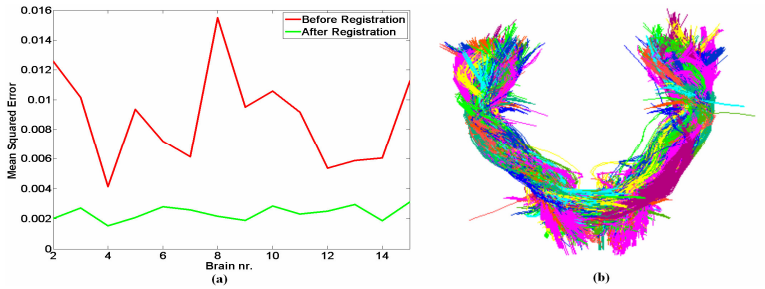

Fig. 5 (a) mean squared error between model and target fibers before (red curve) and after (green curve) registration with the ICF for each brain in the dataset; (b) the 14 target CSTs after their alignment with the model, each color representing another brain from the dataset.

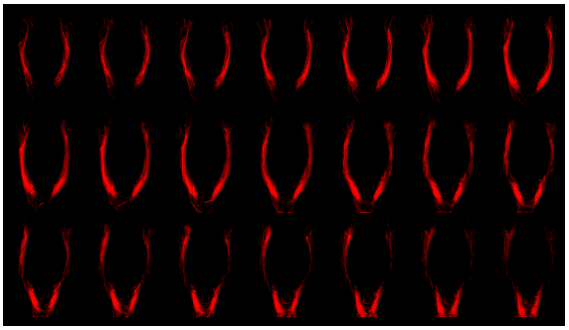

Fig. 6 Coronal slices number 113 (top left) to 133 (bottom right) of the CST atlas.

References

[1] P.J Basser , and C. Pierpaoli. Microstructural and physiological features of tissues elucidated by quantitative- diffusion-tensor MRI. J Magn Reson B, 111(3):209-219, 1996.

[2] S. Mori, and P.C.van Zijl. Fiber tracking: principles and strategies–a technical review. NMR Biomed, 15(7-8):468-480, 2002.

[3] S. Wakana, H. Jiang, M. Nagae-Poetscher, P.C.M. vanZijl, and S. Mori. A fiber-tract based atlas of Human white matter anatomy. Radiology, 230(1):77-87,2004.

[4] H. Jiang, P.C.M. van Zijl, J. Kim, G.D. Pearlson, and S. Mori. DtiStudio: Resource program for diffusion tensor computation and fiber bundle tracking. Comp. Meth. and Prog. Biomed., 81(2):106-116,2006.

[5] P. Fillard, N. Toussaint, and X. Pennec. MedINRIA: DT- MRI Processing and Visualization Software. Guest paper at the Similar Tensor Workshop, Las Palmas, Spain, November 2006.

[6] http://lbam.med.jhmi.edu/.

[7] M. Maddah, and W. E. L. Grimson, and S. Warfield. Statistical Modeling and EM Clustering of White Matter Fiber Tracts. 3rd IEEE International Symposium on Biomedical Imaging: Macro to Nano (ISBI) 2006, 53-56.

[8] L. O'Donnell, and C.-F. Westin. A High-Dimensional Fiber Tract Atlas. International Society of Magnetic Resonance in Medicine (ISMRM), 2006.

[9] P.J. Besl, and N.D. Mckay. A method for registration of 3D shapes. IEEE Trans. Patt. Anal. Mach. Intell., 14(2):239-256, 1992.

[10] N. I. Fisher, and A. J. Lee. Correlation coefficients for random variables on a unit sphere or hypersphere. Biometrika, 73(1):159-164, 1986.

[11] T. Darrell, P. Indyk and G. Shakhnarovich (eds.). Nearest Neighbor Methods in Learning and Vision: Theory and Practice. MIT Press, 2006.

[12] M.A. Fischler, and R.C. Bolles. Random sample consensus: a paradigm for model fitting with application to image analysis and automated cartography. Commun. Assoc. Comp. Mach., 24(6):381-395, 1981.